This article has been accepted for publication in a future issue of this journal, but has not been fully edited. Content may change prior to final publication. Citation information: DOI 10.1109/TAES.2017.2667236, IEEE Transactions on Aerospace and Electronic Systems

PN Ranging Based on Noncommensurate Sampling: Zero-bias Mitigation Methods

Xiaojun Jin, Ning Zhang, *Member, IEEE*, Kan Yang, Xuemin (Sherman) Shen, *Fellow, IEEE*, Zhaobin Xu, Chaojie Zhang, and Zhonghe Jin

***Abstract*—This paper proposes two methods to mitigate the zero-bias of noncommensurate sampling based code tracking loops to significantly improve the pseudo-noise (PN) ranging accuracy. For the compensation-based method, a set of algorithms are developed to directly calculate the zero-bias which is then removed from the range measurement. For the compensation-free method, a special category of sampling ratios are selected such that the zero-bias is self-cancelled. Simulations validate the effectiveness of the proposed methods.**

***Index Terms*—pseudo-noise ranging, code tracking loop, noncommensurate sampling, zero-bias, sampling ratio.**

I. Introduction

PSEDUO-NOISE (PN) code ranging (or called PN ranging) is an important time-of-arrival (TOA) radio ranging method, and is widely used in space applications, such as global navigation satellite systems (GNSS) (e.g., Global Positioning System [1]), formation flying spacecraft [2]–[4] in which a GPS-like signal structure is usually used for inter-spacecraft distance and/or bearing angle measurements, and deep space exploration [5]–[11]. Although the achievable accuracy of PN ranging might not be as high as that of another radio ranging technique-carrier ranging [1], [12]–[14], it is simpler, and can operate independently and in a real-time way. In fact, a centimeter-level PN ranging accuracy, which is sufficiently high for most applications, can be achieved under high SNR conditions and with elaborate design. In addition, a PN ranging sequence can be modulated by low-rate data, known as spread spectrum modulation [2]–[4], or can be coexistent with data transmission using phase modulation [5]–[7], [11], so ranging and communication can be integrated into one channel.

In a PN ranging system, a code tracking loop is commonly employed to measure the time delay of the ranging signal [1], [15]–[18], and digital code tracking loops are often used to replace existing analogue counterparts [19], [20]. However, the code tracking accuracy, owing to digital implementation, is limited at a sample-period level. This means that an extremely high sampling rate is necessary to achieve a high ranging accuracy, which will lead to unacceptably high power consumption and other design difficulties such as electro magnetic compatibility (EMC) and heat dissipation problems. Noncommensurate sampling is an effective solution to this issue [21]–[26], and has been applied in some GPS receivers [27], [28]. In this sampling scenario, a non-integer number of samples per chip is employed to achieve subsample-period time discrimination without using high sampling rate. It has been elucidated in [22] that with noncommensurate sampling, the code tracking accuracy of digital loops can be improved to be comparable to that of analogue loops. However, it was assumed that the time delay discrimination resolution of noncommensurate sampling was infinite and that there were no other error sources except thermal noise. In fact, besides thermal noise, there are two other factors affecting the achievable code tracking accuracy [24]: the chip phase delay discrimination resolution, and the S-curve zero-bias (or called zero bias) of the code tracking loop which results from the nonideality of the autocorrelation curve of practical PN sequences. It has been demonstrated in [24] that the tracking error due to the former factor can be reduced to an expected level by simply improving the chip phase delay discrimination resolution. However, it is not easy to predict and eliminate the S-curve zero bias error. This error can be as large as tens of times of the phase delay discrimination resolution, so it becomes a dominant error under high SNR conditions and cannot be neglected. Although it is possible to reduce the zero bias error by further increasing the chip phase delay discrimination resolution or using multiples of the matching correlation length [24], both these two approaches are at the expense of much longer correlation time (worse real-time performance) and higher design complexity. This poses a great challenge for improving the PN ranging accuracy and to the best knowledge of the authors, this issue has not been addressed in existing literatures.

In this paper, motivated by a precise ranging demand for space applications, we propose two methods to significantly reduce the zero bias error. Specifically,

(i) We propose a compensation-based method to mitigate the zero bias error. In this method, a set of algorithms are developed to calculate the zero bias of the PN code tracking loop. Based on these algorithms, a range measurement processing scheme is devised to remove the zero bias from the measurement;

(ii) We propose a compensation-free zero bias error mitigating method. We find an especial category of sampling ratios, i.e., compensation-free sampling ratios. By selecting

Xiaojun Jin, Zhaobin Xu, Chaojie Zhang and Zhonghe Jin are with Zhejiang University, Hangzhou, China, 301127. Xiaojun Jin is also a visiting scholar at the University of Waterloo, Canada. E-mail: {axemaster, zjuxzb, zhangcj, jinzh}@zju.edu.cn.

Ning Zhang and Xuemin (Sherman) Shen are with the Department of Electrical and Computer Engineering, University of Waterloo, Waterloo, ON, Canada, N2L 3G1. E-mail: {n35zhang, sshen}@uwaterloo.ca.

Kan Yang is with the Department of Computer Science, the University of Memphis, Memphis, USA, TN 38152-3240. E-mail: kane.cryptosec@gmail.com.

This article has been accepted for publication in a future issue of this journal, but has not been fully edited. Content may change prior to final publication. Citation information: DOI 10.1109/TAES.2017.2667236, IEEE Transactions on Aerospace and Electronic Systems

such ratios, the zero bias is inherently self-cancelled and thus compensation is no longer needed;

(iii) Although this paper is mainly motivated by space applications in which multipath effect is not a dominating factor, we also consider the case of small correlation spacings that is often used in PN tracking loops as an important multipath mitigation measure. Hence, this work forms the basis from which extensions to include practical channel impairments can be made especially for ground applications;

(iv) We evaluate the performance of our methods and algorithms through extensive simulations. The simulation results show that with these methods the steady-state error variance can be reduced by about one order of magnitude for different correlation spacings. Furthermore, based on the proposed methods, we present some generalized guidelines for selecting the parameters of noncommensurate sampling.

The remainder of the paper is organized as follows. The system model and the concept of zero bias are introduced in Section II. The zero bias calculation algorithms and the range measurement processing scheme of the compensation-based method are proposed in Section III. Section IV presents the concept of compensation-free ratio and explains how the compensation-free method works. Section V evaluates the performance with extensive simulations. Some further discussion of designing the parameters of noncommensurate sampling is provided in Section VI. Finally, conclusions and future works are given in Section VII.

II. System Description

A. Code Tracking Loop with Noncommensurate Sampling

The model of a simplified digital early-late PN code tracking loop with noncommensurate sampling is illustrated in Fig.1. In PN ranging, the code tracking loop is used for code synchronization, based on which the timing information for range determination is extracted. Code synchronization typically consists of the two sequential operations of acquisition and tracking. During code acquisition, the received signal's code phase is determined to within some rough interval, usually plus or minus half a chip duration; the estimated PN sequence position $\hat{\eta}$ ($\hat{\eta}$ is an integer and $\hat{\eta} \in [1, L_c]$, where L_c is the period of the PN sequence) is thus obtained. Once acquisition is done, the code-tracking process refines this timing synchronization to get a much more accurate estimate of the chip phase, $\hat{\tau}$ ($\hat{\tau} \in [-0.5, 0.5]$). The combination of $\hat{\eta}$ and $\hat{\tau}$, i.e., $\hat{\eta}+\hat{\tau}$, produces the raw range measurement. This measurement can be easily converted to the range by multiplying with cT_c, where c is the radio propagation speed and T_c is the chip period. Here, we mainly focus on the issue of how to improve the estimate accuracy of $\hat{\tau}$ in noncommensurate sampling based code tracking loops.

The transmitted signal is modeled as a PN waveform with rectangular chips of duration T_c. The signal modulates an RF carrier ω_c and is transmitted across the channel, and received at a delay and with a reduced amplitude due to the signal path. The thermal noise in the receiver front end is modeled as an additive white Gaussian noise component with a flat double-sided power spectral density $N_0/2$ Watts/Herz. To clearly demonstrate the effectiveness of the proposed methods, we assume there is no data modulating the PN code and the code is perfectly demodulated in the receiver. Extensions to include data modulation and imperfect carrier estimation can be made based on existing works such as [22]; in fact, the effect of including these factors can be neglected under reasonable conditions [22]. The received baseband ranging signal can be written as

$$r(t) = \sqrt{2P} \sum_{k=-\infty}^{\infty} c_k p(t - kT_c - \tau) + n(t), \tag{1}$$

where P is the ranging signal power, c_k is the PN sequence, $p(t)$ is a unit amplitude rectangle in the interval $[0, T_c]$, τ is the unknown chip phase delay assumed to be uniformly distributed in the interval $[-T_c/2, T_c/2]$, and $n(t)$ is the white Gaussian noise component.

Following the signal path of the early-late loop shown in Fig.1, the received signal is first passed through an ideal low-pass filter with bandwidth W Hz, which models the front-end band-limiting filter and is wide enough to pass the signal undistorted. The signal is subsequently sampled at a rate $1/T_s$. The chip pulse shape is only nonzero when $0 \leqslant mT_s - kT_c - \tau \leqslant T_c$, so the digitalized ranging signal can be expressed as

$$r(mT_s) = \sqrt{2P} c_{\lfloor (mT_s - \tau)/T_c \rfloor} + n_m, \tag{2}$$

where n_m is the digitalized noise component. The sampled signal is delivered to the early and late correlators followed by the loop discriminator, loop filter and code generator. A late minus early discriminator is used and the S-curve function is $0.5(R(\tau - d/2) - R(\tau + d/2))$, where $R(\tau)$ is the autocorrelation function, and d is the correlation spacing of the early-late loop. A correlation spacing of 1 is usually used for general applications, while much smaller ones are often chosen to combat the multipath effect for ground and indoor applications [29]. Based on the estimated chip phase, the local early, prompt and late codes are generated as $c_{\lfloor (mT_s + dT_c/2 - \hat{\tau})/T_c \rfloor}$, $c_{\lfloor (mT_s - \hat{\tau})/T_c \rfloor}$ and $c_{\lfloor (mT_s - dT_c/2 - \hat{\tau})/T_c \rfloor}$ respectively. Therefore, one can obtain the early and late correlations (i.e., the output of the early and late correlators) expressed as

$$\begin{cases} C_e = \sum_{m=0}^{L_m - 1} r(mT_s) c_{\lfloor (mT_s + dT_c/2 - \hat{\tau})/T_c \rfloor} \\ C_l = \sum_{m=0}^{L_m - 1} r(mT_s) c_{\lfloor (mT_s - dT_c/2 - \hat{\tau})/T_c \rfloor}. \end{cases} \tag{3}$$

where L_m is the correlation length, i.e., the number of samples involved in one correlation period.

In noncommensurate sampling, a non-integer sample-period to chip-period ratio $T_s/T_c = N/M$ (or defined as sampling ratio) is used to achieve subsample-period time discrimination, where N and M are mutually prime integers; accordingly, the phase delay discrimination resolution is $1/M$. A specific correlation length called matching correlation length, which is equal to M, is required to match this resolution in order to guarantee the expected accuracy of noncommensurate sampling [24]. Readers are referred to [22]–[24] for more details about noncommensurate sampling.

This article has been accepted for publication in a future issue of this journal, but has not been fully edited. Content may change prior to final publication. Citation information: DOI 10.1109/TAES.2017.2667236, IEEE Transactions on Aerospace and Electronic Systems

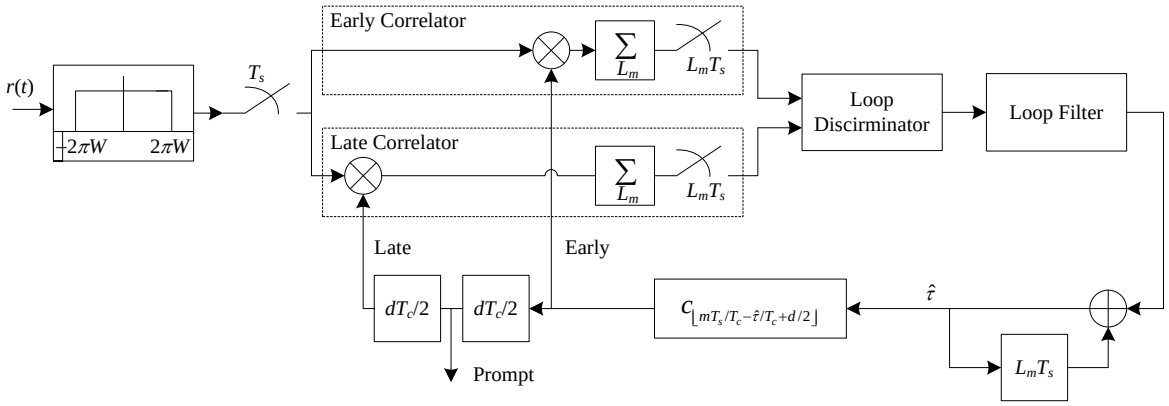

Fig. 1. Digital early-late PN code tracking loop.

B. Zero Bias and Related Factors

For a classical digital early-late code tracking loop using noncommensurate sampling, the loop S-curve zero bias results from the left-right asymmetry of the autocorrelation curve $R(\tau)$. This is shown in Fig.2 and explained as follows. Actual PN code sequences are not ideal square waves, and there are randomly distributed short consecutive 1 (or -1) sub-sequences in a PN sequence. This leads to the appearance of small flat sections on the autocorrelation curve and causes the curve to deviate from the ideal stair-wise shape. Each 1/-1 sub-sequence results in a small flat section, the width of which depends on the length (i.e, the number of chips) of the corresponding 1/-1 sub-sequence. Because of the randomness of the distribution of the 1/-1 sub-sequences in a whole PN code sequence, the distribution of the small flat sections on the autocorrelation curve is also random. This results in the left and right parts of the autocorrelation curve being asymmetric and thus the autocorrelation values at $\tau = d/2$ (i.e., $R(d/2)$) and $\tau = -d/2$ (i.e., $R(-d/2)$) are different (as shown in Fig. 2(a)). Therefore, the early and late correlation values at $\tau = 0$ (i.e., $R_{e0} = R_e(0) = R(d/2)$ and $R_{l0} = R_l(0) = R(-d/2)$) are different (Fig. 2(b)), which in turn leads to the zero bias being nonzero (Fig. 2(c)). This zero bias may be as large as tens of times of the phase delay discrimination resolution, so it cannot be neglected for precise ranging applications. For example, as shown in Fig. 2, the discrimination resolution is $1/1022$ (chip), while the zero bias reaches about 0.02 (chip).

Observing closely the relationship between the shape of the autocorrelation curve and the distribution of the samples on the PN ranging code, we can find that besides the sampling ratio (matched with the matching correlation length) and the used PN sequence, the shape of the autocorrelation curve is also related to two other factors: the sequence position and the chip phase of the first sample, i.e., the initial sequence position and the initial chip phase, of the correlation. As a consequence, the zero bias is also related to these factors.

Furthermore, we can find how the variation of the autocorrelation curve with respect to the phase delay is related to the positions of the involved samples. When we increase the phase delay between two correlated sequences from zero to $d/2$ at $1/M$ per step, at every step there is a new pair of

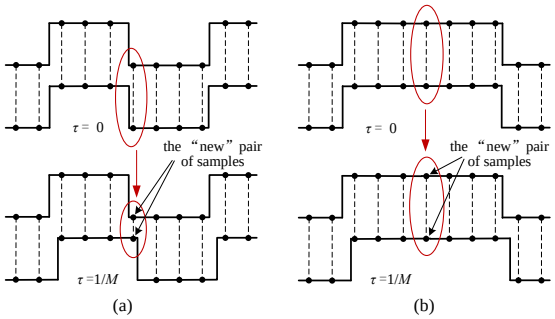

Fig. 3. Two cases of phase delay distinguishment.

samples that can potentially distinguish the increased phase delay. There are two cases regarding whether this pair of samples can indeed distinguish the increased phase delay. As shown in Fig.3(a), if the chip values of the two correlated sequences at this sampling epoch are different, then the pair of samples successfully distinguish the increased phase delay, which makes the correlation value decrease at this step. Conversely, if the chip values are the same, the increased phase delay is not discriminated, which causes the correlation value not to change at this step (Fig.3(b)).

Based on above analysis, it becomes possible to calculate the correlation value $R(\tau)$ of any phase delay τ. In particular, after getting the correlation values R_{e0} and R_{l0}, and hence the S-curve offset, we can further calculate the S-curve zero bias. Before these calculations, however, a key issue is to find the position of the pair of samples that potentially discriminate the phase delay increase/decrease at every step, which will be explained in detail in the next section.

In practice, the correlation period in terms of number of chips, N, is usually designed to be an integer multiple of the PN sequence period L_c to facilitate the implementability of the sampling rate. For example, the sequence period of the GPS C/A codes is 1023, so we need to select an N as 1023, 2046, 3069, etc. It is worth noting that for such N, the zero bias maintains fixed during loop operation, since the distribution of sample positions in every correlation period is exactly the same for a given received PN code. However, the sequence position and chip phase of the received code are unknown and

This article has been accepted for publication in a future issue of this journal, but has not been fully edited. Content may change prior to final publication. Citation information: DOI 10.1109/TAES.2017.2667236, IEEE Transactions on Aerospace and Electronic Systems

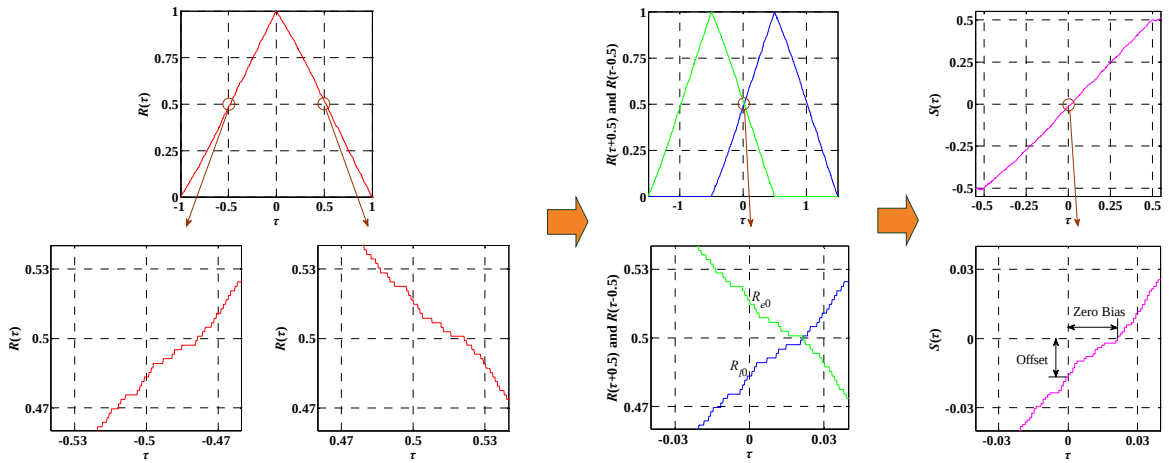

(a) Autocorrelation curve $R(\tau)$ (b) Early (R_e=$R(\tau$+0.5), green) and late (R_l=$R(\tau$-0.5), blue) correlation curves (c) S-curve

Fig. 2. Illustration of the offset and zero bias of the S-curve, d=1. A late minus early discriminator is used and the S-curve function is $S(\tau) = 0.5(R(\tau - 0.5) - R(\tau + 0.5))$. $Offset = S(0) = 0.5(R(-0.5) - R(0.5)) = 0.5(R_{l0} - R_{e0})$. The sampling ratio: $N/M = 1023/1022$. In (a)(b) and (c), the bottom subfigure(s) is(are) obtained by zooming in the top subfigure.

randomly change for different measurement segments (e.g., the received signal loses lock, and then is acquired and measured again.), so we need a generalized method to mitigate the different zero bias of each measurement segment.

The frequently used mathematical notations in this paper are summarized in TABLE I.

TABLE I
FREQUENTLY USED NOTATIONS

Notation	Definition
N/M	Sampling ratio, equals T_s/T_c
$1/M$	Phase delay discrimination resolution
L_m	Correlation length in terms of number of samples
T_s	Sample period
T_c	Chip period
d	Correlation spacing of the early-late loop
P_i, P_i^e, P_i^l	Position of the sample of the current step for calculating the correlation value
P_i^s	Sequence position
P_i^c	Chip phase
P_0, P_0^s, P_0^c	Initial position
L_s	Interval of the two samples respectively involved in two adjacent steps for calculating correlation values
$\lceil x \rceil$	Round x toward positive infinity
$\lfloor x \rfloor$	Round x toward negative infinity
$mod(x, y)$	Modulus operation
c_k	PN sequence value of the k-th chip
L_c	Period of the PN sequence
R_{e0}, R_{l0}	Early and late correlation values at $\tau = 0$
Z	Zero bias
$\hat{\eta}$	Estimated sequence position
$\hat{\tau}$	Estimated chip phase
$\hat{\tau}'$	Compensated estimated chip phase
σ_τ^2	Loop steady-state error variance
P/N_0	Signal to noise ratio (SNR)

III. COMPENSATION-BASED METHOD

In this section, we will present some algorithms for calculating the S-curve zero bias of a noncommensurate sampling based early-late PN code tracking loop. With these algorithms, we can predict the zero bias and remove it from the ranging measurement. The calculation of the zero bias includes two phases: 1) calculation of the early and late correlation values at phase delay of 0, i.e., R_{e0} and R_{l0}, and 2) calculation of the zero bias based on the obtained correlation values. As mentioned in the previous section, before these phases, a critical issue is to seek the position of the next pair of samples based on the position of the current pair of samples at each step.

A. Prediction of Sample Positions

The procedure for calculating correlation values is as follows. Taking the calculation of R_{l0} as an example, it is assumed that the prompt sequence is fixed and the late sequence is moved so that the phase delay of the late sequence with respect to the prompt sequence increases from zero to d/2 at a step size of 1/M chips. At every step, a new pair of samples can potentially contribute to the variation of the correlation value. As illustrated in Fig.3, if this pair of samples can indeed discriminate the increased phase delay, the normalized correlation value decreases by 2/M. Otherwise, the correlation value does not change at this step. After Md/2 steps, R_{l0} is eventually obtained.

Assume that on the prompt sequence, the position interval of the two samples respectively corresponding to two adjacent steps is L_s sample periods, i.e.,

$$P_{i+1} = P_i + L_s N/M, \tag{4}$$

where P_i is the position of the sample corresponding to the

This article has been accepted for publication in a future issue of this journal, but has not been fully edited. Content may change prior to final publication. Citation information: DOI 10.1109/TAES.2017.2667236, IEEE Transactions on Aerospace and Electronic Systems

current step, and $P_i = P_i^s + P_i^c$. P_i^s is the sequence position, which is an integer and satisfies $P_i^s \in [1, L_c]$. P_i^c is the chip phase, which is a decimal and satisfies $P_i^c \in [-0.5, 0.5]$. Our objective is to find L_s to get P_{i+1} given P_i. It is not difficult to find that the value of L_s is fixed for any two adjacent steps. In what follows, the detailed procedure to find L_s is presented.

Since the step size is $1/M$, the chip phase of the sample corresponding to the next step must be $1/M$ larger than that corresponding to the current step, i.e., $P_{i+1}^c = P_i^c + 1/M$. Therefore, the fractional part of $L_s N/M$ must be $1/M$. Based on this fact, one can obtain

$$mod(L_s N, M) = 1, \tag{5}$$

where $mod(x, y)$ is the modulus operator. It is notable that once the sampling ratio is given, L_s can be calculated off-line in advance. For example, L_s is 1 for N/M = 1023/1022, and is 87 for N/M = 1023/1000. After getting L_s, we can obtain P_{i+1} according to (4) and then the corresponding sample value $c_{(mod(\lceil P_{i+1} \rceil, L_c))}$, where $c_{(\cdot)}$ is the PN code sequence.

Similarly, we can calculate R_{e0} by assuming that the phase delay of the early sequence with respect to the prompt sequence decreases from zero to -d/2 at a step size of $1/M$ and using the following equation:

$$P_{i+1} = P_i - L_s N/M. \tag{6}$$

R_{e0} is thus obtained after $Md/2$ steps.

B. Calculation of R_{e0} and R_{l0}

The pseudo code of the proposed algorithm for calculating the correlation values is described in Algorithm 1. The detailed procedure is summarized as follows. Firstly, relevant parameters are initialized including the correlation value and the number of cycles to be executed. In particular, the position of the first sample to be processed is calculated which is equal to the initial position P_0 plus a displacement related to the initial chip phase P_0^c. In each cycle, the chip values of the two correlated sequences at the current concerned sampling epoch are compared to determine whether the phase delay increase is distinguishable by the pair of samples newly involved at the current step; then, the position of the sample corresponding to the next step is updated. Note that every time the sample position is updated, a position adjustment is subsequently needed to guarantee that the sample to be processed is within the range of the correlation period, i.e., $P_i \in [P_0, P_0 + N]$. Mathematically, this operation can be described as

$$P_i = \begin{cases} P_i + N, & P_i < P_0 \\ P_i - N, & P_i > P_0 + N \\ P_i, & else \end{cases}. \tag{7}$$

C. Calculation of Zero Bias

After obtaining R_{e0} and R_{l0} according to Algorithm 1, we are ready to calculate the zero bias. Different from the procedure used in the calculation of correlation values, here we assume that the early and late sequences are fixed and the prompt sequence is moved along time by $1/M$ chips per step until the early and late correlation values, R_e and R_l, are equal. The eventual number of moved steps is exactly the calculation result of the zero bias. As illustrated in Fig. 4, for example, if R_e is greater than R_l, the prompt code is moved right to reduce the difference between the two correlation values (increase the late correlation value and decrease the early correlation value).

The pseudo code of the proposed algorithm for calculating the zero bias is described in Algorithm 2. Notably, the initial values of R_e and R_l are the output of Algorithm 1, and ϵ is a sufficiently small number, e.g., $1/M$.

Algorithm 1 Calculation of R_{e0} and R_{l0}.

Input: $R_{e0} = R_{l0} = 1$, number of cycles $loop = floor(Md/2)$, initial position $P_1^l = P_0 + \lceil -P_0^c M \rceil \cdot N/M \cdot L_s$ and $P_1^e = P_0 + \lfloor -P_0^c M \rfloor \cdot N/M \cdot L_s$ with position adjustment.

Output: R_{e0}, R_{l0}.

```
Calculate R_l0
for i = 1 : loop do
    c_p = c_{mod(⌈P_i^l⌉, L_c)};
    c_l = c_{mod(⌈P_i^l − d/2⌉, L_c)};
    if c_p ≠ c_l then
        R_l0 = R_l0 − 2/M;
    end if
    Update P_{i+1}^l according to (4);
    Position adjustment;
end for
Calculate R_e0
for i = 1 : loop do
    c_p = c_{mod(⌈P_i^e⌉, L_c)};
    c_e = c_{mod(⌈P_i^e + d/2⌉, L_c)};
    if c_p ≠ c_e then
        R_e0 = R_e0 − 2/M;
    end if
    Update P_{i+1}^e according to (6);
    Position adjustment;
end for
return R_e0 and R_l0.
```

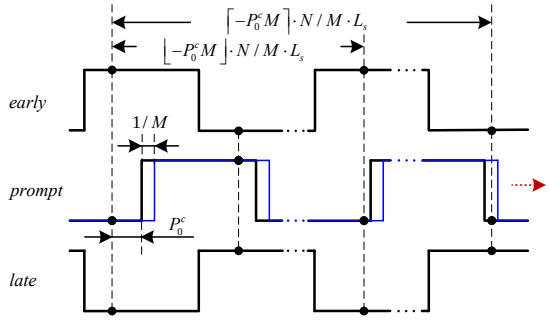

Fig. 4. Illustration of the calculation of the zero bias.

D. Range Measurement Processing

Based on Algorithm 1 and Algorithm 2, we propose a processing scheme for PN ranging measurement. We assume

This article has been accepted for publication in a future issue of this journal, but has not been fully edited. Content may change prior to final publication. Citation information: DOI 10.1109/TAES.2017.2667236, IEEE Transactions on Aerospace and Electronic Systems

Algorithm 2 Calculation of the zero bias.

Input: $R_e = R_{e0}$ and $R_l = R_{l0}$, initial zero bias $Z = 0$, initial position $P_1^l = P_0 + \lceil -P_0^c M \rceil \cdot N/M \cdot L_s$ and $P_1^e = P_0 + \lfloor -P_0^c M \rfloor \cdot N/M \cdot L_s$ with position adjustment. $i = 1$.

Output: Z.

```
if R_e > R_l then
  while (R_e − R_l) > ε do
    Z = Z + 1/M;
    c_p = c_{mod(⌈P_i^e − Z⌉, L_c)};
    c_l = c_{mod(⌈P_i^e − d/2⌉, L_c)};
    if c_p ≠ c_l then
      R_e = R_e − 2/M;
      R_l = R_l + 2/M;
    end if
    Update P_{i+1}^e according to (6);
    Position adjustment;
    i = i + 1;
  end while
else
  while (R_l − R_e) > ε do
    Z = Z − 1/M;
    c_p = c_{mod(⌈P_i^l − Z⌉, L_c)};
    c_e = c_{mod(⌈P_i^l + d/2⌉, L_c)};
    if c_p ≠ c_e then
      R_e = R_e + 2/M;
      R_l = R_l − 2/M;
    end if
    Update P_{i+1}^l according to (4);
    Position adjustment;
    i = i + 1;
  end while
end if
return The zero bias Z.
```

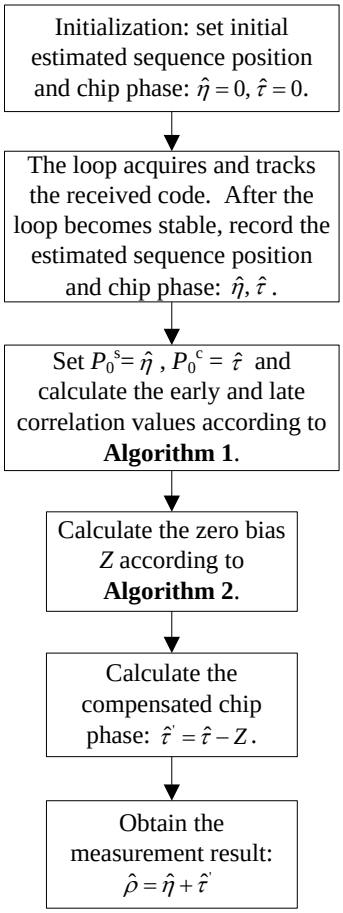

Fig. 5. Range measurement processing flow in the receiver.

that a noncommensurate sampling based digital early-late PN code tracking loop with a correlation spacing d is employed in the receiver of the PN ranging system, and that the time synchronization between the transmitter and the receiver has been completed. The processing flow is summarized in Fig. 5. Note that after the loop locks the ranging code and becomes stable, the estimated sequence position $\hat{\eta}$ and estimated chip phase $\hat{\tau}$ are delivered as inputs to the two algorithms.

IV. Compensation-free method

After having a clear understanding of the distribution pattern of the samples on the PN ranging code in one correlation period for a given sampling ratio, we can also find that there exists a special category of sampling ratios which are associated with the correlation spacing d. With such ratios (called compensation-free ratios), almost the same set of sequence chips are sampled for the early and late correlations, leading to R_{e0} and R_{l0} almost the same. As a consequence, the zero bias is almost completely self-cancelled and any compensation is no longer needed. It is notable that such a compensation-free ratio is once used in [28]. However, the authors in [28] didn't explain how it worked and didn't put forward a generalized approach of how to choose such ratios. To address this issue, we present the following theorem for selecting compensation-free sampling ratios.

Theorem 1: For a correlation spacing d of $1/2^j$, where j is a nonnegative integer, there exist compensation-free sampling ratios of $1/2^{j+1} \pm 1/M$, where $1/M$ is the designed phase delay discrimination resolution. The maximum residual zero bias caused by the compensation-free ratio itself is $1/M$ chips if the S-curve function is $0.5(R(\tau - d/2) - (\tau + d/2))$.

Proof: Take the scenario when $d = 1 (j = 0), M = 40$ and the corresponding compensation-free ratio $N/M = 21/40$ as an example. The sequence positions and chip phases of all samples within one correlation period are shown in Fig. 6(a). We can see that one half of the samples fall into the chip phase interval [0, 0.5), which means that these samples are involved in the calculation of R_{l0} according to Algorithm 1; the other half of the samples are within the chip phase interval [-0.5, 0), and these samples are involved in the calculation of R_{e0}. More importantly, both halves of the samples traverse almost the same set of chips, i.e., all chips except chip 11 are sampled in the chip phase interval [-0.5, 0), while all chips except chip 1 are sampled in the chip phase interval [0, 0.5]. In other words, there are two samples on almost every chip and these two samples are involved in the early and late correlation respectively. Therefore, R_{e0} and R_{l0} are almost the same according to algorithm 1, which results in the zero bias being

This article has been accepted for publication in a future issue of this journal, but has not been fully edited. Content may change prior to final publication. Citation information: DOI 10.1109/TAES.2017.2667236, IEEE Transactions on Aerospace and Electronic Systems

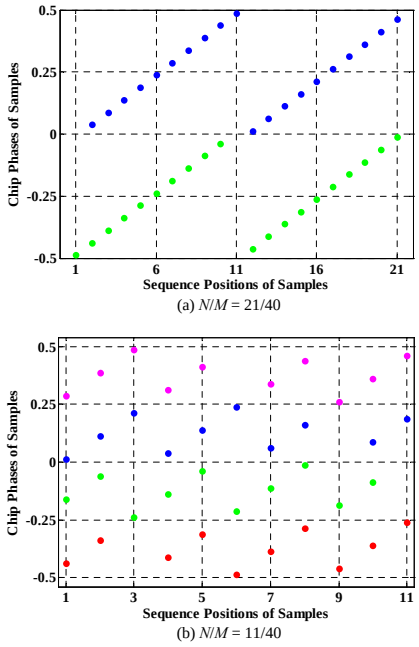

(a) N/M = 21/40

(b) N/M = 11/40

Fig. 6. Illustration of the principle of compensation-free ratios. In (a), all chips except chip 11 are sampled in the chip phase interval [-0.5, 0), and all chips except chip 1 are sampled in the chip phase interval [0, 0.5). In (b), all chips expect chip 11 are sampled in the chip phase interval [-0.25, 0), and all chips except chip 9 are sampled in the chip phase interval [0, 0.25).

nearly zero. Similarly, if $d = 1/2(j = 1)$, then we can select an compensation-free sampling ratio of $1/4 \pm 1/M$, as demonstrated in Fig. 6(b). To be more accurate, for compensation-free ratios $1/2^{j+1} \pm 1/M$, there are 2^{j+1} chips that only have one sample, and among these chips one chip is involved in the early correlation and another involved in the late correlation, so the difference between the two normalized correlation values can be 0 or $\pm 2/M$. As a result, the zero bias is not more than $1/M$ since $S(\tau) = 0.5(R(\tau - d/2) - R(\tau + d/2))$ is satisfied. ■

V. Performance Evaluation

A. Residual Error Analysis

Residual error sources of the compensation-based method include 4 items: thermal noise, phase delay discrimination resolution $1/M$, calculation errors of the algorithms, and the error related to short consecutive 1/-1 subsequences existing in PN codes. The impact of thermal noise on the loop tracking accuracy has been investigated in [22]. The magnitude of the error due to a finite phase delay discrimination resolution can be obtained as

$$\sigma_M^2 = \int_{-M/2}^{M/2} \frac{1}{M} \cdot x^2 \cdot dx = \frac{1}{12M^2}(chips^2), \qquad (8)$$

where the chip phase of the received ranging code is considered to follow a uniform distribution. As we can observe in Algorithm 1 and Algorithm2, the maximum calculation errors are both $1/M$ approximately.

The last error item, which can be called sequence irregularity error, appears when a small flat section is exactly located on the horizontal axis of the loop S-curve. Apparently, the error magnitude directly depends on the width of the flat section. There are two cases concerning whether the flat section is directly related to a consecutive 1/-1 sub-sequence. If L_s, mentioned in (4), is equal to 1, the flat section is directly related to a consecutive 1/-1 sub-sequence. In other words, the longer the length of this sub-sequence, the wider the flat section, and in turn the larger the sequence irregularity error. In this case, therefore, we can select PN sequences with short consecutive 1/-1 sub-sequences to reduce this error. Otherwise, if L_s is larger than 1, the flat section is not associated with a specific consecutive 1/-1 sub-sequence, so this measure does not necessarily work.

For the compensation-free method, the error sources are similar and the only difference is that the sampling ratio itself introduces an error of not more than $1/M$ chips, as described in Theorem 1, instead of the algorithm errors.

Another important factor that needs to be mentioned is the chip rate. As a fundamental relationship, the achievable tracking accuracy is inversely proportional to the chip rate [1]. In the following evaluation, the GPS C/A code which uses a length-1023 Gold sequence at a chip rate of 1.023Mcps, specifically pseudo-random noise code 1 (PRN 1), will be used unless otherwise noted.

B. Numerical Results of Offset

1) Offset Variation for Different Initial Positions: Before simulation, it's necessary to have a clear insight into the magnitude of the zero bias prior to compensation and how it varies with respect to the related parameters. We focus on the offset of the S-curve (i.e., $0.5(R_{l0} - R_{e0})$, as shown in Fig. 2(c)) rather than the zero bias for two main reasons. Firstly, the magnitude of the offset is so small for compensation-free ratios that the calculation of the zero bias will be inaccurate. Secondly, it is easy and straightforward to numerically calculate the offset, while loop simulation is necessary to obtain the zero bias, which will be too time-consuming if all possible values of related parameters are simulated. Focusing on the offset instead will not affect the effectiveness of the following numerical results, since the offset and the zero bias approximately conform to a one-to-one mapping relationship.

As mentioned earlier, given the PN code sequence and the sampling ratio (matched with the matching correlation length), the shape of the S-curve only depends on the initial sequence position and initial chip phase of the correlation. Fig. 7 shows the relationship between the (normalized) offset and the initial sequence position/initial chip phase for sampling ratio 1023/1022 prior to compensation. We can see that before compensation, the maximum offset is at a 10^{-2} level, which cannot be neglected for precise ranging applications. However, as shown in Fig. 8, for the compensation-free ratio 1023/2044, the offset is always less than 0.5×10^{-3} (not more than $1/M = 1/2044$).

Furthermore, from Fig.7, it can also be seen that the offset of one sequence position is a phase-shifted version of that of another sequence position. This can be mathematically expressed by

This article has been accepted for publication in a future issue of this journal, but has not been fully edited. Content may change prior to final publication. Citation information: DOI 10.1109/TAES.2017.2667236, IEEE Transactions on Aerospace and Electronic Systems

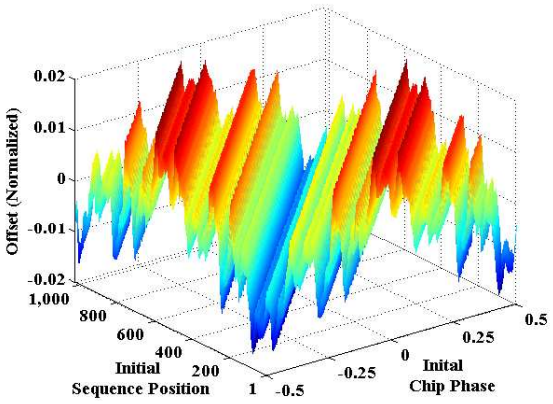

Fig. 7. Offsets for N/M=1023/1022, d = 1, and PN sequence of PRN 1.

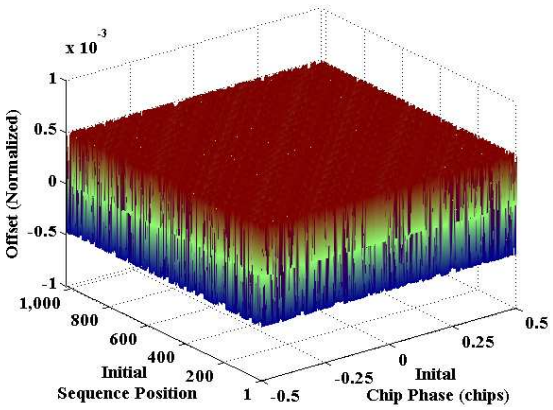

Fig. 8. Offsets for N/M=1023/2044, d = 1, and PN sequence of PRN 1.

$$Offset(P_0^s, P_0^c) = Offset(1, P_0^s/L_c - 1/2 - P_0^c), \quad (9)$$

where $P_0^s/L_c - 1/2 - P_0^c$ should be adjusted when it is out of the range of P_0^c, i.e., [-0.5, 0.5). Therefore, we only need to concentrate on the offset of one sequence position for the sake of distinct demonstration, and in the rest of the paper we will only consider the case of P_0^s =1.

Fig. 9 shows the variation of the offset with respect to the chip phase for different sampling ratios. It can be seen that the offset of $N/M = 1023/1022$ can be as large as nearly 0.02, and the offset of the sampling ratio with larger M ($N/M = 3069/3068$) is approximately proportionally reduced. The offset of a compensation-free ratio $N/M = 1023/2044$ is also shown in this figure, and we can see that the magnitude of the offset is considerably smaller than that of $N/M = 3069/3068$, even with a smaller M (2044 versus 3068); the maximum offset is 1/2044, which is consistent with the theoretical analysis. The same result can be observed for compensation-free ratios used to match correlation spacings less than 1, as shown in Fig. 10.

2) Offset Variation during Loop Operation: It is necessary to verify the offset variation during loop operation, as the S-curve may change from one correlation period to another, and Fig.9-10 only show the S-curves of one period. The offsets of 200 consecutive correlation periods for different sampling ratios are cut out from a running loop that has entered the tracking status. From Fig.11, we can see that as expected the offset maintains fixed and the magnitude is only related to the initial position P_0, for both the non-compensation-free ratio and the compensation-free ratio.

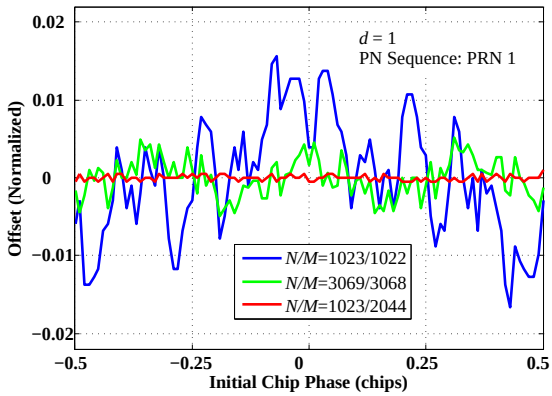

Fig. 9. Offsets for different sampling ratios.

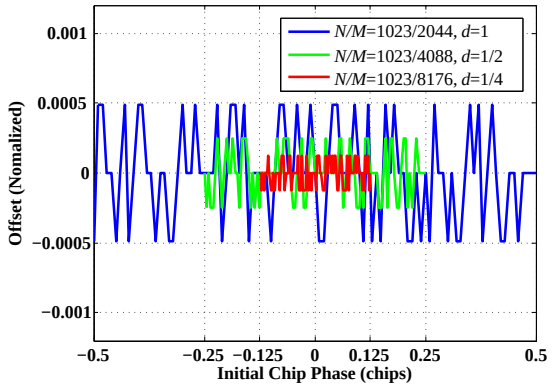

Fig. 10. Offsets for compensation-free ratios corresponding to different correlation spacings.

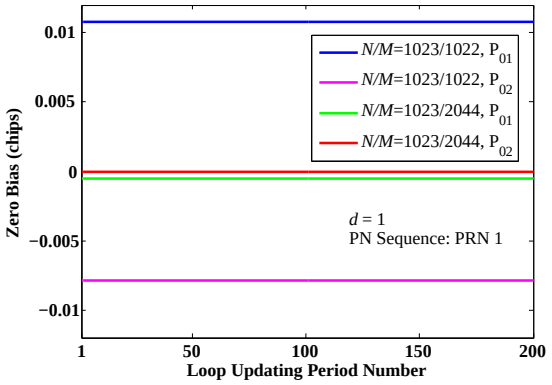

Fig. 11. Offset variation during loop operation.

C. Simulation Results

1) Simulation Setup: We will focus on the loop tracking performacne at high SNRs so that the effect of thermal noise can be neglected and the effectiveness of the proposed methods can be clearly observed, since this work is motivated by precise

This article has been accepted for publication in a future issue of this journal, but has not been fully edited. Content may change prior to final publication. Citation information: DOI 10.1109/TAES.2017.2667236, IEEE Transactions on Aerospace and Electronic Systems

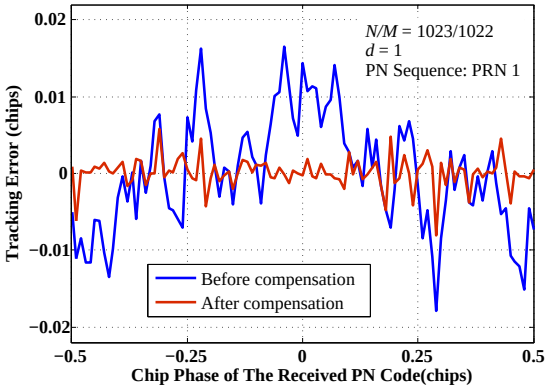

Fig. 12. Compensation result for $d = 1$.

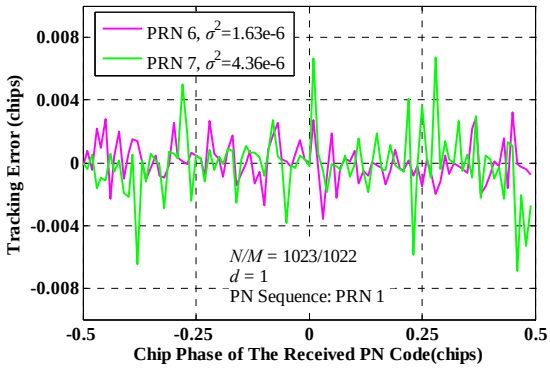

Fig. 13. Compensation results for different PN sequences.

ranging applications. Monte-Carlo simulations with a SNR range of 60-80 dBHz, a loop bandwidth (B_L) of 1 Hz and a frontend bandwidth (W) of $1/T_c$ are run using MATLAB. To take into account the effect of the initial chip phase, a received PN ranging code with 100 different randomly generated initial chip phases is delivered to the code tracking loop and the obtained measurement results are subsequently averaged. The initial sequence position is fixed on 1, since the impact of the initial sequence position is equivalent to that of the initial chip phase as indicated by (9). In addition, different correlation spacings and different PN sequences are used in the simulation to examine their impact on the performance.

2) Compensation Results for Different Initial Chip Phases: Before evaluating the tracking accuracy, we firstly verify the effectiveness of the proposed compensation-based method for different initial chip phases. We follow the range measurement processing flow as described in Fig.5. Thermal noise is not added to the ranging signal so that the verification results can be clearly observed. Fig.12 shows the tracking error versus the chip phase of the received PN code. It can be seen that the zero bias is considerably reduced through compensation. Moreover, it can also be seen that after compensation the residual zero bias of some chip phases are still relatively prominent. This is because relatively large sequence irregularity errors are suffered corresponding to these chip phases. As mentioned previously, for sampling ratios with $L_s = 1$, we can select PN sequences with short consecutive 1/-1 sub-sequences to reduce the sequence irregularity error. In Fig.13, the residual zero biases of two different PN sequences are compared. We can see that the difference is obvious, which validates the importance of selecting an appropriate PN sequence. Some statistics of consecutive 1/-1 subsequences of these two PN sequences are also provided in TABLE II.

In Fig.14, the compensation result for a correlation spacing less than 1 is demonstrated. As we can see in this figure, the compensation is also effective.

3) Loop Tracking Performance: The loop steady-state tracking performance is simulated for two sampling ratios with different phase delay discrimination resolutions to examine the achievable accuracy of the compensation-based method. The results are shown in Fig.15, and there are several points we need to notice. First, in the relatively low SNR region,

TABLE II
STATISTICS OF CONSECUTIVE 1/-1 SUBSEQUENCES

Item	PRN 6	PRN 7
Number of consecutive 1 or -1 sub-sequences with length of 6 or more	6	20
Number of consecutive 1 or -1 sub-sequences with length of 7 or more	6	12
Number of consecutive 1 or -1 sub-sequences with length of 8 or more	2	8
Length of the longest consecutive 1 or -1 subsequence	9	12

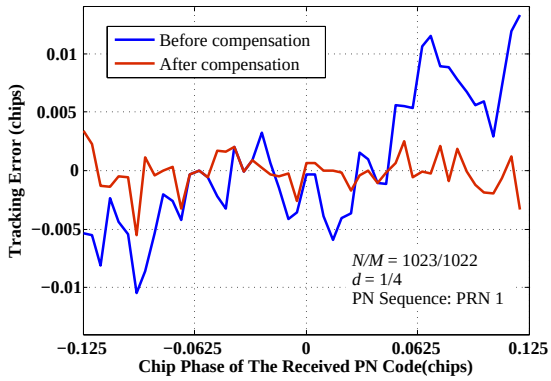

Fig. 14. Compensation result for d less than 1.

the tracking accuracy is more dependent on thermal noise. In the high SNR region, however, other error sources are dominant, leading to the curve becoming flat, which reveals the achievable accuracy under high SNR conditions. Second and most importantly, the steady-state error variance is significantly reduced through compensation, by at least one order of magnitude. In other words, the correlation time can be shortened by 3-4 times for the same tracking accuracy, so the real-time performance can be enhanced. Finally, the tracking accuracy is approximately proportionally improved by using sampling ratios with smaller $1/M$. This means that the phase delay discrimination resolution is a decisive factor of the achievable accuracy. The reason is that although there exist other errors, they are reduced accordingly when the phase delay discrimination resolution is improved. It is noticeable

This article has been accepted for publication in a future issue of this journal, but has not been fully edited. Content may change prior to final publication. Citation information: DOI 10.1109/TAES.2017.2667236, IEEE Transactions on Aerospace and Electronic Systems

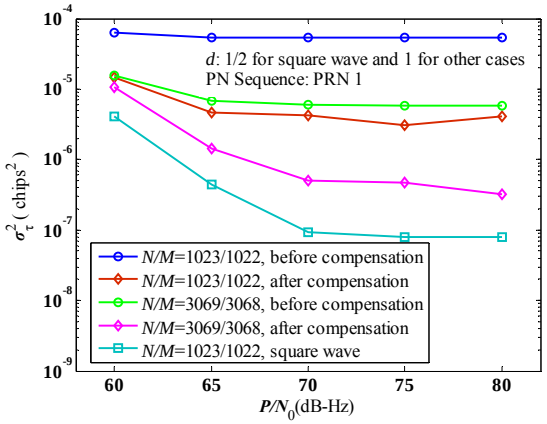

Fig. 15. Steady-state error variances for sampling ratios with different M.

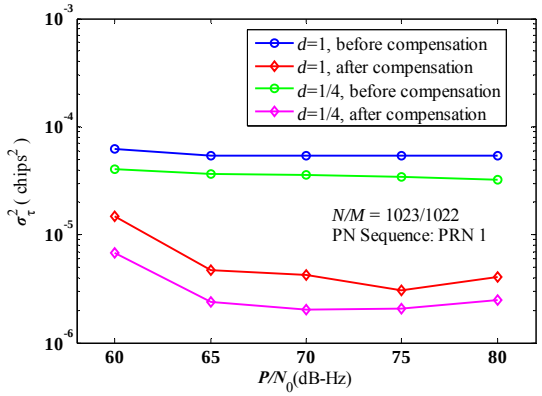

Fig. 16. Steady-state error variances for different d.

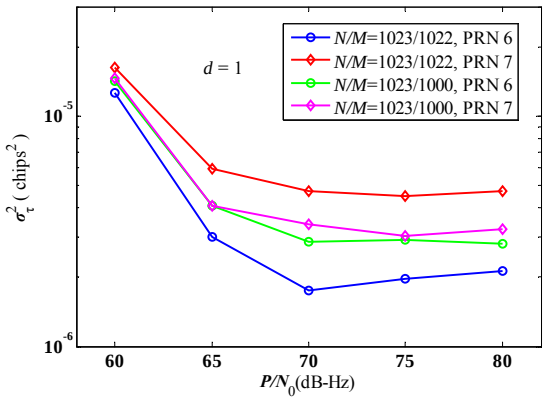

Fig. 17. Steady-state error variances of different PN sequences after compensation.

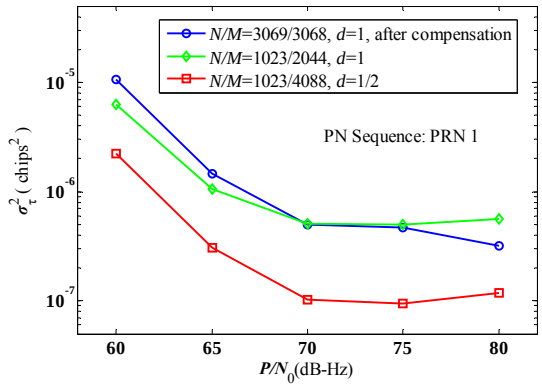

Fig. 18. Tracking performance comparison between compensation-based and compensation-free methods.

that a sufficiently high SNR of the ranging signal is necessary to guarantee the effectiveness of increasing M. For example, as indicated in Fig. 15, a SNR of at least 65 dB-Hz is expected for $N/M = 1023/1022$, while the SNR needs to be at least 70 dB-Hz for $N/M = 3069/3068$.

The tracking performance of a square wave is also simulated as a benchmark, the error sources of which only include thermal noise and the phase delay discrimination resolution. As shown in Fig.15, the achieved steady-state error variance well accords with the theoretical result provided by (8), which justifies the correctness of our simulations. In addition, we can see that the performance inferiority of the PN sequence over the square wave is still quite large, even if the compensation is used. This is mainly because of the sequence irregularity error as illustrated in Fig. 12. Note that a correlation spacing of 1/2 is used since for a square wave, the effective phase delay range of the autocorrelation curve is 1 rather than 2.

Fig. 16 shows the steady-state error variance for a correlation spacing less than 1. It can be seen that the tracking error are also dramatically reduced through compensation. In addition, the tracking accuracy is higher for smaller d. This is because for smaller d, less number of samples are involved in the correlations, which results in less accumulated difference between R_{e0} and R_{l0}.

Fig. 17 shows the tracking performance of two PN sequences with quite large difference in statistics of consecutive 1/-1 subsequences. We can see that for the sampling ratio 1023/1022 with $L_s = 1$, the tracking accuracy of the PN sequence with shorter consecutive 1/-1 subsequences is apparently superior over that of the other sequence. This validates the importance of selecting appropriate PN sequences. However, for the sampling ratio 1023/1000 with $L_s = 87$, the performance difference is much less apparent, which accords with the previous analysis.

Fig.18 shows the benefit of using compensation-free ratios. The tracking performance of the compensation-free ratio ($N/M = 1023/2044$) in high SNR region is similar to that of the non-compensation-free ratio ($N/M = 3069/3068$) after compensation, even with a lower phase delay discrimination resolution (1/2044 versus 1/3068). This indicates that we can give priority to using the compensation-free method rather than the compensation-based method. In addition, similar to what is indicated in Fig.15, the tracking accuracy of compensation-free ratios is approximately proportionally improved by using ratios with smaller $1/M$.

Fig. 19 and Fig. 20 shows the tracking accuracy at a particular SNR for three non-compensation-free sampling ratios and three compensation-free ratios, respectively. It can be seen that centimeter-level accuracy can be achieved by selecting appropriate phase delay discrimination resolutions. If there still exists a large gap between the required and achievable

This article has been accepted for publication in a future issue of this journal, but has not been fully edited. Content may change prior to final publication. Citation information: DOI 10.1109/TAES.2017.2667236, IEEE Transactions on Aerospace and Electronic Systems

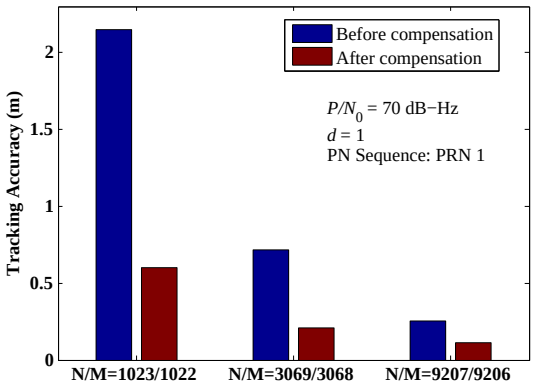

Fig. 19. Tracking accuracy for non-compensation-free ratios.

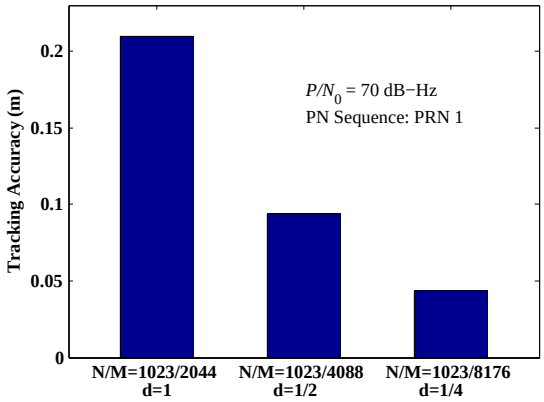

Fig. 20. Tracking accuracy for compensation-free ratios.

performance, higher chip rates can be considered since the tracking accuracy is inversely proportional to the chip rate [1]. We will not go deep into this issue since the loop noise performance is not the focus of this work.

VI. Further discussion

Based on the two proposed methods, we recommend some guidelines for designing the parameters of noncommensurate sampling for high accuracy PN ranging applications. Suppose that a high ranging SNR is guaranteed and the chip rate, the correlation spacing d (1 for general applications and 1/2, 1/4, 1/8 etc. for multipath mitigation purpose) and the allowed correlation time are given. In addition, PN sequences with short consecutive 1/-1 subsequences are chosen. As mentioned in Section II, N should be an integer multiple of the period of the PN sequence, L_c , to guarantee the implementability of the sampling rate. We arrange these guidelines into a design flow as follows.

1) Step 1: Select a range of the phase delay discrimination resolution according to the required code tracking accuracy. As indicated by the simulation results, the achievable code tracking accuracy is approximately proportional to the phase delay discrimination resolution $1/M$. As a starting point, we can choose a discrimination resolution to be higher than half the required code tracking accuracy (in chips).
2) Step 2: Give priority to the compensation-free method, i.e., select sampling ratios corresponding to the correlation spacing d according to Theorem 1. Specifically, select $1/2 \pm 1/M$ for general applications, and $1/2^{j+1} \pm 1/M$ corresponding to $d = 1/2^j (j > 0)$ for multipath mitigation.
3) Step 3: If any compensation-free ratio is unavailable due to design constraints on the sampling rate, we can choose non-compensation-free sampling ratios and use the compensation-based method to mitigate the zero bias. If the compensation-free ratio is available but the correlation spacing is too small leading to an unacceptably high sampling rate, we also need to choose the compensation-based method.
4) Step 4: When choosing a non-compensation-free ratio, we should consider a ratio with a relatively small integer part to avoid excessively long correlation time; meanwhile, to lower the effect of consecutive 1/-1 subsequences and to avoid high power consumption incurred by a high sampling rate, we should not select too small ratios. As a compromise, we could select sampling ratios as close to 1 as possible, e.g., 0.5-2.0.
5) Step 5: Determine N based on the selected possible sampling ratios.

In summary, the compensation-free method is more preferred, as no compensation is needed and the design complexity can be lowered. However, it is not as generalized as the compensation-based method, since it is only valid for a particular category of sampling ratios. Moreover, a too high sampling rate will be demanded if a very small correlation spacing is desired for multipath mitigation, which may result in unacceptably high power consumption. In these cases, non-compensation-free ratios should be chosen and the compensation-based method be utilized. Overall, we should choose one of these two methods according to different practical system requirements and constraints.

VII. Conclusion

In this paper, two methods have been proposed to mitigate the zero bias error existing in noncommensurate sampling based digital PN code tracking loops. In the compensation-based method, a set of algorithms are brought forward to calculate the zero bias, based on which a range measurement processing scheme is presented to remove the zero bias from the measurement. In the compensation-free method, a special type of sampling ratios, compensation-free ratios, are found with which the zero bias is self-cancelled, as the samples involved in the early and late correlations reside on almost the same set of sequence chips. Simulation results demonstrate that with the proposed methods, the zero bias can be significantly reduced and thus the PN ranging accuracy can be greatly improved for different correlation spacings. Finally, some design guidelines are provided for determining the parameters of noncommensurate sampling and selecting one of these two methods according to different system requirements. The work of this paper can be extended to applications in which practical impairments such as multipath and Doppler effects need to be considered.

ACKNOWLEDGMENT

This research work is supported by the National Natural Science Foundation of China (Grant No. 60904090 and 61401389), the National Science Foundation for Distinguished Young Scholars of China (Grant No. 61525403), and the Natural Sciences and Engineering Research Council (NSERC) of Canada. Xiaojun Jin is also financially supported by the China Scholarship Council.

REFERENCES

[1] E. Kaplan and C. Hegarty, *Understanding GPS: Principles and Applications*. Artech House, 2006.

[2] J.-B. Thevenet and T. Grelier, "Formation flying radio-frequency metrology validation and performance: The PRISMA case," *Acta Astronautica*, vol. 82, pp. 2–15, 2013.

[3] M. Delpech, P. Guidotti, T. Grelier, D. Seguela, J. Berges, S. Djalal, and J. Harr, "First formation flying experiment based on a radio frequency sensor: lessons learned and perspectives for future missions," in *International Conference on Spacecraft Formation Flying Missions and Technologies*, 2011, pp. 1–9.

[4] R. Sun, "Relative navigation for satellite formation flying based on radio frequency metrology," Ph.D. dissertation, May 2014.

[5] CCSDS, "Pseudo-noise (PN) ranging systems," *Recommended standard: CCSDS 414.1-B-2 Blue Book*, Feb. 2014.

[6] J. Berner, S. Bryant, and P. Kinman, "Range measurement as practiced in the deep space network," *Proc. IEEE*, vol. 95, no. 11, pp. 2202–2214, 2007.

[7] G. Boscagli, P. Holsters, E. Vassallo, and M. Visintin, "PN regenerative ranging and its compatibility with telecommand and telemetry signals," *Proc. IEEE*, vol. 95, no. 11, pp. 2224–2234, 2007.

[8] M. Maffei, L. Simone, and G. Boscagli, "On-board PN ranging acquisition based on threshold comparison with soft-quantized correlators," *IEEE Trans. Aero. Elec. Sys.*, vol. 48, no. 1, pp. 869–890, 2012.

[9] J. L. Massey, G. Boscagli, and E. Vassallo, "Regenerative pseudo-noise (PN) ranging sequences for deep-space missions," *Int. J. Satellite Commun. Network.*, vol. 25, no. 3, pp. 285–304, 2007.

[10] ——, "Regenerative pseudo-noise-like (PNL) ranging sequences for deep-space missions," *Int. J. Satellite Commun. Network.*, vol. 25, no. 3, pp. 305–322, 2007.

[11] C. B. Haskins, D. J. Duven, C. C. DeBoy, and J. R. Jensen, "First deep-space flight demonstration of regenerative pseudo-noise ranging," in *IEEE Aero. Conf.*, 2012, pp. 1–6.

[12] T. Bandikova, J. Flury, and U.-D. Ko, "Characteristics and accuracies of the GRACE inter-satellite pointing," *Advances in Space Research*, vol. 50, no. 1, pp. 123–135, 2012.

[13] S. Asmar, A. Konopliv, M. Watkins, J. Williams, R. Park, G. Kruizinga, M. Paik, D.-N. Yuan, E. Fahnestock, D. Strekalov, N. Harvey, W. Lu, D. Kahan, K. Oudrhiri, D. Smith, and M. Zuber, "The scientific measurement system of the gravity recovery and interior laboratory (GRAIL) mission," *Space Science Reviews*, vol. 178, no. 1, pp. 25–55, 2013.

[14] C. Wang and M. Zhou, "Novel approach to intersatellite distance measurement with high accuracy," *J. Guid. Contrl Dynam.*, vol. 38, no. 5, pp. 944–948, 2015.

[15] T. Kao and J. Juang, "Weighted discriminators for GNSS BOC signal tracking," *GPS Solutions*, vol. 16, no. 3, pp. 1–13, 2011.

[16] J.-C. Juang and T.-L. Kao, "Noncoherent BOC signal tracking based on a five-correlator architecture," *IEEE Trans. Aero. Elec. Sys.*, vol. 48, no. 3, pp. 1961–1974, 2012.

[17] E. Falletti, B. Motella, and M. T. Gamba, "CSC code discriminator: theoretical analysis of performance," *J. Inst. Navig.*, vol. 62, no. 1, pp. 39–54, 2015.

[18] S. Zitounia, K. Rouabahb, D. Chikouchec, K. Mokranie, S. Atiab, R. Harbaf, and P. Ravierf, "General analytical models characterizing MBOC modulated signal," *Aerospace Science and Technology*, vol. 50, pp. 112–126, 2016.

[19] W. Zhuang and J. Tranquilla, "Digital baseband processor for the GPS receiver - modeling and simulation," *IEEE Trans. Aero. Elec. Sys.*, vol. 29, no. 4, pp. 1343–1349, 1993.

[20] ——, "Modeling and analysis for the GPS pseudo-range observable," *IEEE Trans. Aero. Elec. Sys.*, vol. 31, no. 2, pp. 739C–751, 1995.

[21] A. Mileant, S. Million, S. Hinedi, and U. Cheng, "The performance of the all-digital data transition tracking loop using nonlinear analysis," *IEEE Trans. Commun.*, vol. 43, no. 2–4, pp. 1202–1215, 1995.

[22] K. J. Quirk and M. Srinivasan, "PN code tracking using noncommensurate sampling," *IEEE Trans. Commun.*, vol. 54, no. 10, pp. 1845–1856, 2006.

[23] X. Jin, C. Zhang, Z. Jin, J. Jiang, , and W. Yang, "Pseudo-noise code regeneration based on noncommensurate sampling and dynamic clock phase shifting," *Electron. Lett.*, vol. 46, no. 16, pp. 1126–1127, 2010.

[24] X. Jin, Z. Xu, C. Zhang, and Z. Jin, "Simple approach to determining parameters of noncommensurate sampling for optimal pseudo-noise code phase delay discrimination," *Electron. Lett.*, vol. 50, no. 4, pp. 283–284, 2014.

[25] D. M. Akos and M. Pini, "Effect of sampling frequency on GNSS receiver performance," *J. Inst. Navig.*, vol. 53, no. 2, pp. 85–95, 2006.

[26] C. J. Hegarty, "Analytical model for GNSS receiver implementation losses," in *Proceedings of the 22nd International Technical Meeting of The Satellite Division of the Institute of Navigation (ION GNSS 2009)*, 2009, pp. 3165–3178.

[27] J. B. Thomas, "Functional description of signal processing in the Rogue GPS receiver," Jet Propulsion Lab., Pasadena, CA,USA, Tech. Rep. JPL Publication 88-15, Jun. 1988.

[28] ——, "Signal-processing theory for the TurboRogue receiver," Jet Propulsion Lab., Pasadena, CA,USA, Tech. Rep. JPL Publication 95-6, Apr. 1995.

[29] A. J. Van Dierendonck, P. Fenton, and T. Ford, "Theory and performance of narrow correlator spacing in a GPS receiver," *J. Inst. Navig.*, vol. 39, no. 3, pp. 2139–2154, 1992.

Xiaojun Jin received his Ph.D.degree from Zhejiang University, Zhejiang, China in 2007. Now he is an associate professor of Zhejiang University. He was a visiting researcher with the Broadband Communications Research Laboratory, Department of Electrical and Computer Engineering, University of Waterloo, Canada. His research interests include precise radio ranging, relative navigation for distributed spacecraft systems, and GNSS based localization and navigation.

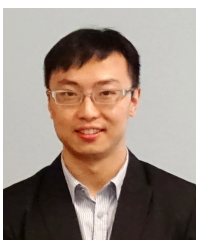

Ning Zhang [S'12, M'16] earned the Ph.D degree from University of Waterloo in 2015. He received his B.Sc. degree from Beijing Jiaotong University and the M.Sc. degree from Beijing University of Posts and Telecommunications, Beijing, China, in 2007 and 2010, respectively. Since then, he has been a postdoc research fellow at BBCR lab in University of Waterloo. His current research interests include next generation wireless networks, software defined networking, green communication, and physical layer security.

This article has been accepted for publication in a future issue of this journal, but has not been fully edited. Content may change prior to final publication. Citation information: DOI 10.1109/TAES.2017.2667236, IEEE Transactions on Aerospace and Electronic Systems

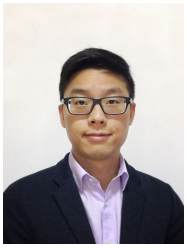

Kan Yang is an assistant professor in Dept. of Computer Science at the University of Memphis. He received his B. Eng. degree in Information Security from University of Science and Technology of China in 2008 and his PhD degree in Computer Science from City University of Hong Kong in August 2013. From Sept. 2013 to July 2014, he was a postdoctoral fellow in the Dept. of Computer Science at the City University of Hong Kong. From July 2014 to June 2016, he was a postdoctoral fellow, the coordinator of security group, at the Broadband Communications Research (BBCR) group in the Dept. of Electrical and Computer Engineering at University of Waterloo, Canada. His research interests include Cloud Security, Big Data Security, Mobile Security, Applied Cryptography, and Distributed Systems.

Xuemin (Sherman) Shen [M'97, SM'02, F'09] received the B.Sc.(1982) degree from Dalian Maritime University (China) and the M.Sc. (1987) and Ph.D. degrees (1990) from Rutgers University, New Jersey (USA), all in electrical engineering. He is a Professor and University Research Chair, Department of Electrical and Computer Engineering, University of Waterloo, Canada. He is also the Associate Chair for Graduate Studies. Dr. Shens research focuses on resource management in interconnected wireless/wired networks, wireless network security, social networks, smart grid, and vehicular ad hoc and sensor networks. He is an elected member of IEEE ComSoc Board of Governor, and the Chair of Distinguished Lecturers Selection Committee. Dr. Shen served as the Technical Program Committee Chair/Co-Chair for IEEE Globecom'16, Infocom'14, IEEE VTC'10 Fall, and Globecom'07, the Symposia Chair for IEEE ICC'10, the Tutorial Chair for IEEE VTC'11 Spring and IEEE ICC'08, the General Co-Chair for ACM Mobihoc'15, Chinacom'07 and QShine'06, the Chair for IEEE Communications Society Technical Committee on Wireless Communications, and P2P Communications and Networking. He also serves/served as the Editor-in-Chief for IEEE Network, Peer-to- Peer Networking and Application, and IET Communications; an Associate Editor-in- Chief for IEEE Internet of Things Journal, a Founding Area Editor for IEEE Transactions on Wireless Communications; an Associate Editor for IEEE Transactions on Vehicular Technology, Computer Networks, and ACM/Wireless Networks, etc.; and the Guest Editor for IEEE JSAC, IEEE Wireless Communications, IEEE Communications Magazine, and ACM Mobile Networks and Applications, etc. Dr. Shen received the Excellent Graduate Supervision Award in 2006, and the Outstanding Performance Award in 2004, 2007, 2010, and 2014 from the University of Waterloo, the Premiers Research Excellence Award (PREA) in 2003 from the Province of Ontario, Canada, and the Distinguished Performance Award in 2002 and 2007 from the Faculty of Engineering, University of Waterloo. Dr. Shen is a registered Professional Engineer of Ontario, Canada, an IEEE Fellow, an Engineering Institute of Canada Fellow, a Canadian Academy of Engineering Fellow, a Royal Society of Canada Fellow, and a Distinguished Lecturer of IEEE Vehicular Technology Society and Communications Society.

Zhaobin Xu was born in 1984.He received his B.E. and Ph.D.degrees from Zhejiang University, Zhejiang, China in 2008 and 2013, respectively. Now he is a lecturer of Zhejiang University. He is a member of Micro-Satellite Research Center. His research interests include micro-satellite communication and navigation systems.

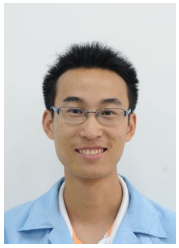

Chaojie Zhang was born in 1982.He received his B.E. and Ph.D.degrees from Zhejiang University, Zhejiang, China in 2004 and 2009, respectively. Now he is a lecturer of Zhejiang University. He is a member of Micro-Satellite Research Center. His research interests include micro satellite and software defined radio technologies.

Zhonghe Jin received his Ph.D. degree in microelectronics and solid-electronics from Zhejiang University, Zhejiang, China in 1998. Currently, he is a professor in Micro-Satellite Research Center, Zhejiang University. His research interests include micro satellite, optical sensors and MEMS/NEMS technologies.